

****FULL TITLE****
*ASP Conference Series, Vol. **VOLUME**, **YEAR OF PUBLICATION***
****NAMES OF EDITORS****

Supernova VLBI

Norbert Bartel

York University, Toronto, ONT, M3J1P3, Canada

Abstract. We review VLBI observations of supernovae over the last quarter century and discuss the prospect of imaging future supernovae with space VLBI in the context of VSOP-2. From thousands of discovered supernovae, most of them at cosmological distances, ~ 50 have been detected at radio wavelengths, most of them in relatively nearby galaxies. All of the radio supernovae are Type II or Ib/c, which originate from the explosion of massive progenitor stars. Of these, 12 were observed with VLBI and four of them, SN 1979C, SN 1986J, SN 1993J, and SN 1987A, could be imaged in detail, the former three with VLBI. In addition, supernovae or young supernova remnants were discovered at radio wavelengths in highly dust-obscured galaxies, such as M82, Arp 299, and Arp 220, and some of them could also be imaged in detail. Four of the supernovae so far observed were sufficiently bright to be detectable with VSOP-2. With VSOP-2 the expansion of supernovae can be monitored and investigated with unsurpassed angular resolution, starting as early as the time of the supernova's transition from its opaque to transparent stage. Such studies can reveal, in a movie, the aftermath of a supernova explosion shortly after shock breakout.

1. Introduction

A supernova (SN), the explosion of a star, is one of the most energetic single events in the universe. Thousands of optical SNe are now known but most of them are at cosmological distances. Only ~ 50 have been detected at radio wavelengths and 12 observed with VLBI, the most distant at almost 100 Mpc. In addition, several SNe and supernova remnants (SNRs) were discovered at radio wavelengths in dust-obscured galaxies, such as M82, Arp 299, and Arp 220, and observed with VLBI. All of the SNe observed with VLBI are thought to have resulted from the core collapse of a massive progenitor and emit synchrotron radiation generated from the electrons accelerated in the region where the shock front interacts with the circumstellar medium (CSM) left over from the wind of the mass-losing progenitor. In addition, some of the radiation may come from the environment of the stellar corpse, a neutron star or a black hole left over from the explosion. During the early stage of the expansion of a radio SN, the radio lightcurve rises quickly because of the decreasing optical depth due to synchrotron self-absorption or to thermal absorption in the ionized CSM along the line of sight. It reaches its peak, first at high frequencies later at lower frequencies, when the optical depth decreases below unity, and it declines thereafter during the optically thin stage of the SN while the SN is expanding (e.g., Chevalier 1982).

For a typical shock front expansion velocity of $10,000 \text{ km s}^{-1}$, the angular size of a SN at a distance of 4 Mpc expands at a rate of 1 mas yr^{-1} . With global

VLBI and a wavelength of 4 cm, an angular resolution of ~ 0.6 mas can be obtained, allowing detailed investigations of the expanding SN and the making of a movie. Global VLBI with VSOP-2 promises to increase the angular resolution at this wavelength to 0.2 mas and to a correspondingly higher resolution at shorter wavelengths, enabling us to witness the aftermath of the explosion shortly after shock breakout.

2. Why supernova VLBI?

The high angular resolution of VLBI affords us the following possibilities:

1. The determination of the morphology. A shell morphology indicates the interaction of the ejecta with the CSM. A centrally-condensed morphology can indicate the presence of a central source, such as a pulsar wind nebula or a black hole accretion disk system. A disk-like morphology suggests an optically thick object, as is expected in the early stages of evolution.
2. The measurement of the angular size, θ , which can give us the average expansion velocity. It helps unravel whether synchrotron self-absorption played a dominant role in the early evolution of the SN, and could reveal any possible presence of a relativistically expanding afterglow of a gamma ray burst (GRB).
3. The measurement of the expansion as a function of time, t , since shock breakout, parametrized by $\theta(t) \propto t^{m(t)}$, which can give us the SN's age and deceleration parameter, $m(t)$.
4. Monitoring the expansion of the SN, which provides information on the density of the ejecta and the CSM, and on the magnetic field, as a function of radius. Obtaining the density profile of the CSM is like a "time machine" that reveals the last thousands of years of the mass-loss history before the star died.
5. A geometric determination of the distance to the SN and its host galaxy using the ESM (expanding shock front method).
6. The making of a movie showing the evolution of the SN.

3. Supernovae observed with VLBI

Supernova VLBI started with observations of SN 1979C in 1982 (Bartel 1985; Bartel et al. 1985) shortly after the new, sensitive, MKIII VLBI data acquisition system became available. Since then 11 more optically identified SNe have been observed with VLBI (Table 1). Eight are Type II, whose progenitors are massive supergiants. Four are Type Ib/c, whose progenitors are believed to be the cores of massive stars which have lost their envelopes. A few Type Ib/c SNe were found to be associated with GRBs. The sources in M82, Arp 299, and Arp 220 are not optically identified but are likely also SNe of Type II or Ib/c or SNRs. The distances range from 50 kpc for SN 1987A to almost 100 Mpc for SN 2003L. Their peak flux densities at 8 GHz reached values of 100 mJy and more, corresponding to very high brightness temperatures. Such SNe are examples for future targets of VLBI with VSOP-2.

About 80% or more of all VLBI observations focussed on just three SNe: SN 1979C, SN 1986J, and SN 1993J. They were sufficiently bright and extended that detailed images could be obtained and, for the latter two, movies made.

Table 1. Characteristics of supernovae observed with VLBI

| Name | Type | Host Galaxy | Distance (Mpc) | S_{8GHz}^1 (mJy) | t_{peak}^2 (yr) | θ_{peak}^3 (mas) | Reference ⁴ |
|-----------|------|---------------|-------------------|-----------------------|----------------------|----------------------------|------------------------|
| SN 1979C | II | M100 | 15 | 7 | 0.9 | 0.30 | 1 |
| SN 1980K | II | NGC 6946 | 6 | 2 | 0.27 | <0.21 | 2 |
| SN 1986J | II | NGC 891 | 10 | 100 | 2.7 | 1.6 | 3 |
| SN 1987A | II | LMC | 0.05 | 80 | 0.005 | 1.5 | 4 |
| SN 1993J | II | M81 | 4 | 100 | 0.27 | 0.55 | 5 |
| SN 1996cr | II | Circinus Gal. | 4 | 150 | 2.7 | 2.8 | 6 |
| SN 2001em | Ib/c | NGC 7112 | 80 | 2 | 2 | 0.11 | 7 |
| SN 2001gd | II | NGC 5033 | 13 | 4 | 0.5 | 0.16 | 8 |
| SN 2003L | Ib/c | NGC 3506 | 92 | 3 | 0.2 | 0.01 | 9 |
| SN 2004et | II | NGC 6946 | 6 | 2 | 0.13 | >0.14 | 10 |
| SN 2007gr | Ib/c | NGC 1058 | 10 | $\lesssim 1$ | ? | ? | 11 |
| SN 2008D | Ib/c | NGC 2770 | 27 | 3 | 0.04 | 0.01 | 12 |
| SN/SNR | ? | M82 | 4 | ? | ? | ? | 13 |
| SN/SNR | ? | Arp 299 | 40 | ? | ? | ? | 14 |
| SN/SNR | ? | Arp 220 | 77 | ? | ? | ? | 15 |

Notes:

¹ The approximate peak flux density of the radio lightcurve measured at 8 GHz or extrapolated from lower frequencies.

² The approximate time after shock breakout when the 8-GHz radio lightcurve peaked, i.e., when the optical depth decreased to below unity. If t_{peak} was not measured at 8 GHz, it is assumed to be $0.7 \times t_{peak}$ at 5 GHz. For items 1 and 2, see references (last column) and/or K. Weiler's home page at <http://rsd-www.nrl.navy.mil/7213/weiler/sne-home.html>.

³ The approximate size of the SN at time t_{peak} extrapolated from the size and expansion given in the references. For SN 1987A, an expansion velocity of 35,000 kms^{-1} is taken (Gaensler et al. 2007). For the Type Ib/c SNe, for which only upper limits of sizes and expansions were available, an expansion velocity of 10,000 kms^{-1} is assumed.

⁴ Latest, or latest comprehensive publications: 1) Bartel & Bietenholz (2003); 2) Bartel (1985); 3) Bietenholz et al. (2004); 4) Jauncey et al. (1988); 5) Bartel et al. (2000); 6) Bauer et al. (2008); 7) Bietenholz & Bartel (2007); 8) Pérez-Torres et al. (2005); 9) Soderberg et al. (2005); 10) Martí-Vidal et al. (2007); 11) Paragi et al. (2007); 12) Soderberg et al. (2008); 13) Beswick et al. (2006); 14) Neff et al. (2004); 15) Lonsdale et al. (2006). Also, see these references or references in there for the characteristics in the table.

In the remainder we will first focus on these three SNe. Then we will discuss the other optically identified SNe and the unidentified SNe/SNRs and lastly address prospects for space VLBI in the context of VSOP-2.

4. Supernovae with detailed VLBI images

4.1. SN 1993J

SN 1993J in M81 is, after SN 1987A, the most intensely observed SN ever. It provides an exemplary case to witness, with increasing relative angular resolution, the evolution of a SN over time. VLBI observations started ~ 30 d after shock breakout (Marcaide et al. 1994; Bartel et al. 1994) and showed that the SN expanded almost freely early on (Bartel et al. 1994). A first detailed image was obtained only several months later after the SN had expanded sufficiently (Marcaide et al. 1995a, see also, Bartel et al. 1995). Fig. 1 shows an example of

a sequence of images of the expanding shell of the SN (Bietenholz et al. 2003, see Marcaide et al. 1995b for an earlier sequence).

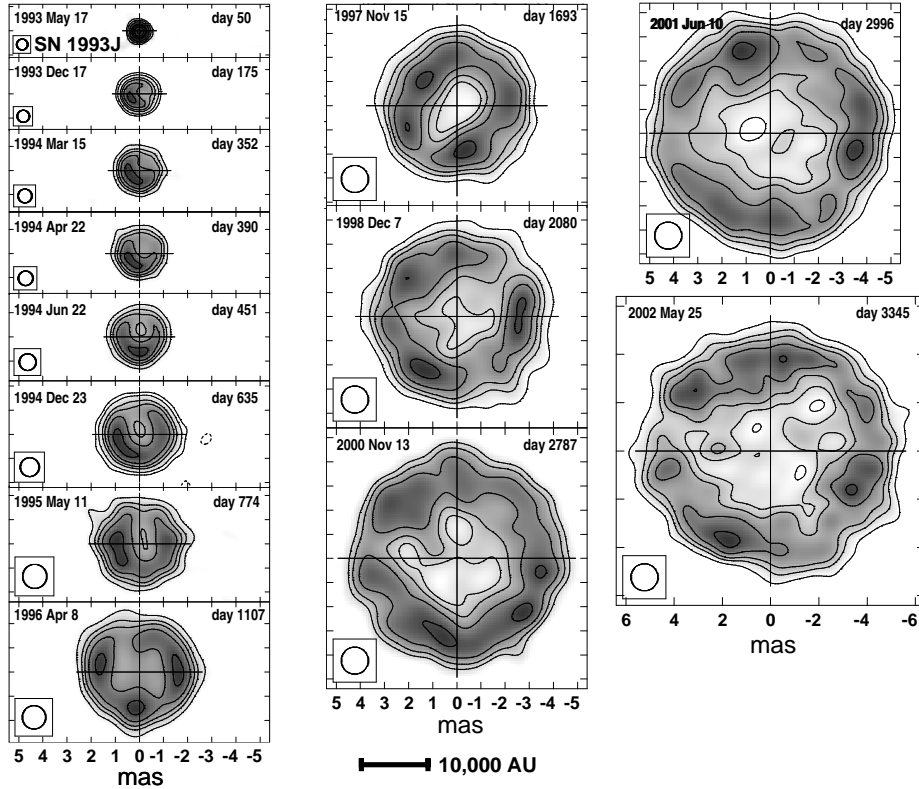


Figure 1. A sequence of 8.4-GHz VLBI images of SN 1993J from $t = 50$ to 3345 d after shock breakout (Bietenholz et al. 2003). The contours are at $-1, 1, 2, 4, \dots, 32, 45, 64,$ and 90% of the peak brightness. For images here and hereafter, the scale on the vertical axis is the same as that on the horizontal axis, the restoring beam is plotted in the lower left, and north is up and east to the left. (To download SN VLBI movies, please visit: <http://www.yorku.ca/bartel>.)

The explosion occurred at a location pinpointed with 160 AU accuracy in the galactic reference frame of the host galaxy M81. From there, the SN expanded isotropically to within 5.5% (Bietenholz et al. 2001).

Initially, the SN expanded rapidly with a velocity of $\sim 20,000 \text{ km s}^{-1}$. Then it was found that the expansion decelerated slightly (Marcaide et al. 1997) and that the deceleration changed over time, t , (Fig. 2, left panel; Bartel et al. 2000, 2002) with the velocity decreasing to $\sim 10,000 \text{ km s}^{-1}$. These measurements are fairly consistent with a hydrodynamic model (Mioduszewski et al. 2001) and provide insight into the physical interplay between the ejecta and the CSM, and the mass-loss history of the progenitor (Bartel et al. 2002).

SN 1993J provided also the best example of geometrically determining a distance using the expanding shock front method (ESM). The distance is derived to be 3.96 ± 0.29 Mpc (Fig. 2, right panel), which, when compared with Cepheid distances, is somewhat larger than Freedman et al. (1994)'s value of 3.63 ± 0.34 Mpc but comparable to Huterer et al. (1995)'s value of 3.93 ± 0.26 Mpc.

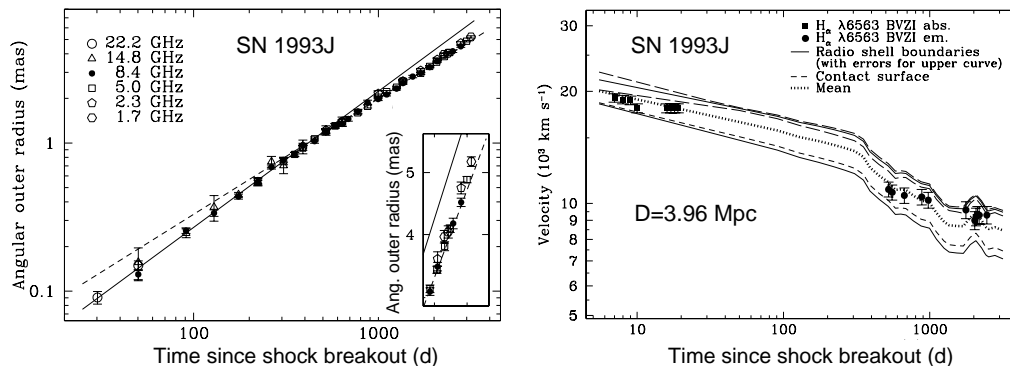


Figure 2. Left: The expansion of SN 1993J. The straight lines give fits which show the changing deceleration of the expansion with $\theta \propto t^{0.919 \pm 0.019}$ for the solid line and $\theta \propto t^{0.781 \pm 0.009}$ for the dashed line. The inset gives a zoomed-in version of the latest part of the expansion curve (Bartel et al. 2002). Right: The velocity of the forward and reverse shocks (outer and inner radio shell) with their mean fit to the maximum $H\alpha$ line velocities, giving the distance to SN 1993J and M81 as indicated in the figure (Bartel et al. 2007).

4.2. SN 1986J

SN 1986J in NGC 891 is an intriguing extragalactic SN, the first one for which a compact component was found to emerge in the projected center of the expanding shell, ~ 20 years after the explosion. It was also the first optically identified SN for which a detailed image could be obtained (Bartel et al. 1991). A series of images is shown in Fig. 3. The new component has a spectrum which was inverted between 5 and 20 GHz when first discovered. The peak is slowly moving to lower frequencies. The inverted part of the spectrum can be interpreted as being due to free-free absorption within the SN shell with the absorption weakening as the shell expands. The new component could be radio emission associated with accretion onto a black hole or the nebula formed around an energetic young neutron star in the center of SN 1986J, which would be the first direct link of a black hole or a neutron star to a modern SN. Its spectral luminosity between 14 and 43 GHz is ~ 200 times that of the Crab Nebula, which is in the range expected for young pulsar wind nebulae (Bandiera et al. 1984). However, since the new component is in the center only in projection, it could also be caused by the interaction of the shock with a particularly dense CSM condensation at the far or near end of the shell. The expansion of the SN is moderately decelerated (see, Fig 3, lower right panel).

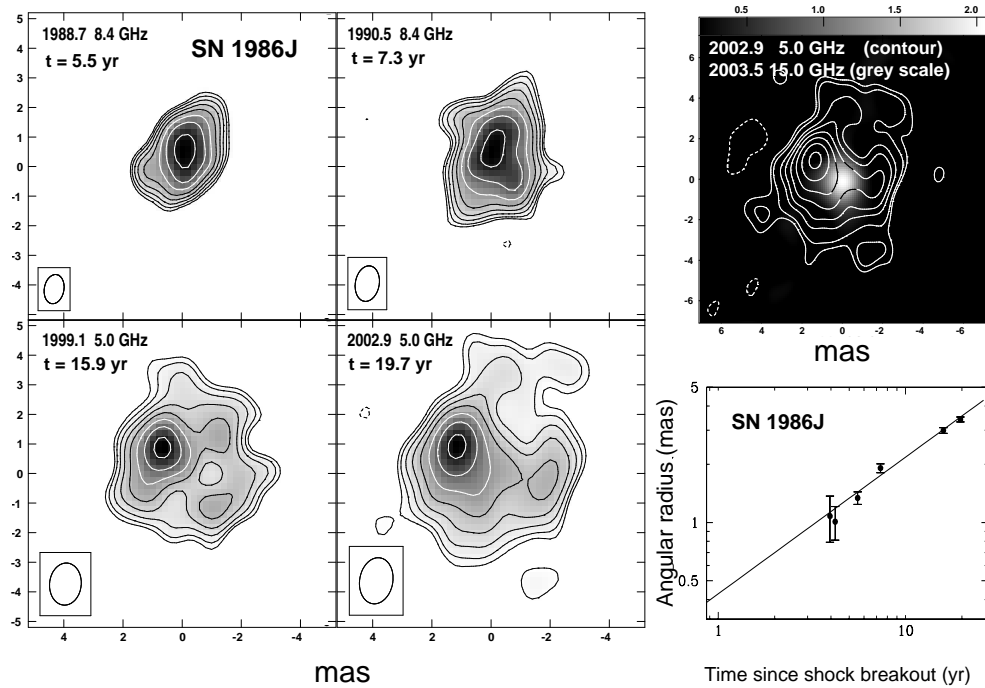


Figure 3. Left: A series of VLBI images of SN 1986J from 1988.7 to 2002.9 with observing frequency and time after shock breakout (1983.2) indicated. The contours are at $-8, 8, 11.3, 16, 22.6, 32, \dots$, and 90.5% of the peak brightness. Top right: A 15-GHz image from 2003.5 showing the central component in grey scale and the 5-GHz image from 2002.9 in (slightly different) contours, in the same reference frame. Bottom right: The expansion of SN 1986J with a best fit of $\theta \propto t^{0.71 \pm 0.11}$ (Bietenholz et al. 2005).

4.3. SN 1979C

SN 1979C in M100 in Virgo has been studied since 1982, and because of its distance of ~ 15 Mpc could only recently be resolved well enough to reveal its shell-like structure (Fig. 4, left panel; Bartel & Bietenholz 2008). The most interesting characteristic is that its expansion is consistent with being almost free up to $t \sim 20$ yr (Fig. 4, right panel). However, significant deceleration may start around this time. From fits to the radio lightcurve, a relatively high progenitor mass-loss rate of 1 to $2 \times 10^{-4} M_{\odot} \text{ yr}^{-1}$ for a wind velocity of 10 km s^{-1} was estimated (Weiler et al. 1991; Montes et al. 2000). However, the kinetic energy of the SN explosion would have to be $\sim 2 \times 10^{52}$ erg to sweep up the mass that corresponds to such mass-loss, more than an order of magnitude larger than is thought appropriate. The mass-loss rate is therefore likely an order of magnitude smaller. Estimates of mass-loss to wind-velocity ratios from radio lightcurve fittings may therefore have to be interpreted with caution (Bartel & Bietenholz 2003).

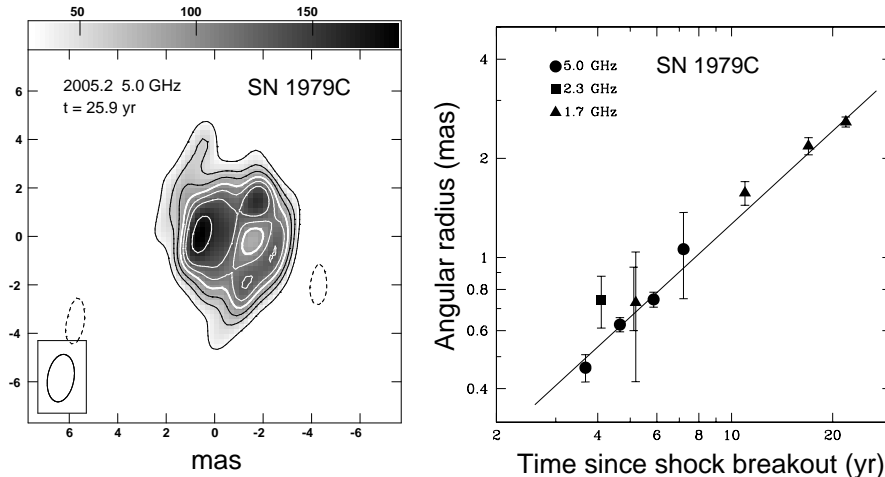


Figure 4. Left: A 5.0-GHz VLBI image of SN 1979C at $t = 25.9$ yr. The contour levels are at $-17, 17, 30, 40, 50$ (emphasized), $60, 70$, and 90% of the peak brightness of $186 \mu\text{Jy bm}^{-1}$. The grey scale, in $\mu\text{Jy bm}^{-1}$, is given at the top (Bartel & Bietenholz 2008). Right: The expansion of SN 1979C with a best fit of $\theta \propto t^{0.94 \pm 0.03}$ for a shell model (Bartel & Bietenholz 2003).

5. Other optically identified supernovae

The only other optically identified SN for which detailed images could be obtained is SN 1987A in the LMC. The images were not obtained with VLBI, but rather with the Australia Telescope Compact Array (ATCA). SN 1987A is by far the closest SN that has ever been observed with VLBI. Its radio lightcurve peaked at ~ 80 mJy, but when VLBI observations were made in a heroic effort $t = 5$ d after shock breakout, the SN was already completely resolved. Nevertheless, a lower limit on the expansion velocity of $19,000 \text{ km}^{-1}$ could be derived (Jauncey et al. 1988). In fact, the SN expanded with a velocity of $\gtrsim 35,000 \text{ km}^{-1}$ and slowed down to 3600 to 5200 km^{-1} for $t > 1800$ d, consistent with the progenitor being a blue supergiant. SN 1987A has a fairly round shell or ring-like morphology with a modulated brightness around the ridge (Manchester et al. 2002; Gaensler et al. 2007).

For the other optically identified SNe, no detailed images could be obtained. Four of them are Type II. SN 1980K and SN 2004et in NGC 6946 were observed only once with VLBI. The angular size of SN 1980K was determined to be $\lesssim 2.0$ mas for a shell model (Bartel 1985) corresponding to an average expansion velocity of $\lesssim 11,000 \text{ km}^{-1}$. For SN 2004et a marginally resolved image, with an indication of an asymmetric brightness distribution, and a lower expansion velocity limit of $15,700 \pm 2000 \text{ km}^{-1}$ was obtained, and it was inferred that synchrotron self-absorption is not relevant for this SN (Martí-Vidal et al. 2007). For SN 2001gd a size of 0.37 ± 0.08 mas was obtained a couple of years after the explosion (Pérez-Torres et al. 2005). Similarly, for SN 1996cr a preliminary size of 10 mas was determined, which helped in the interpretation of this SN as possibly being related to SN 1987A (Bauer et al. 2008).

The remaining four are Type Ib/c SNe. For SN 2007gr, only a detection with VLBI was reported (Paragi et al. 2007). For the others, SN 2001em, SN 2003L, and SN 2008D, upper limits on sizes with corresponding upper limits on average expansion velocities were obtained. For the latter two SNe, these upper limits are relativistic (Soderberg et al. 2005, 2008). For SN 2003L, at 92 Mpc the most distant of the SNe in Table 1, the upper limit helped to distinguish between absorption models, suggesting a (model-dependent) non-relativistic nature of the SN (Soderberg et al. 2005). For SN 2001em, a non-relativistic limit of the expansion velocity could be determined directly. The SN was considered to possibly be related to a GRB event but with a misaligned relativistic jet (Granot & Ramirez-Ruiz 2004). However, VLBI measurements of an expansion velocity of only $5800 \pm 10,000 \text{ km s}^{-1}$ and a proper motion velocity of only $33,000 \pm 34,000 \text{ km s}^{-1}$ disfavor this possibility (Bietenholz & Bartel 2007).

6. Optically unidentified supernovae and supernova remnants

There are a few dust-obscured starburst galaxies with compact radio sources that were found to be SNe or SNRs: M82 (Beswick et al. 2006), Arp 299 (Neff et al. 2004), Arp 220 (Lonsdale et al. 2006). In two other galaxies, NGC 6240 (Gallimore & Beswick 2004), and Mrk 273 (Bondi et al. 2005), compact radio sources were found with VLBI, which are also thought to be possibly SNe or SNRs. The most and longest studied are those in M82. Two sources could be imaged at several epochs. The weaker one, 43.31+592, was found to be shell-type. It expands with a velocity of $9000\text{--}11,000 \text{ km s}^{-1}$, which is typical for SNe. The strongest of all compact sources in M82, 41.95+575, however, is puzzling. The earliest clearly resolved images suggested a shell-like structure, albeit quite elongated with two components at opposite ends (Bartel et al. 1987; Wilkinson & de Bruyn 1990). Recently, an expansion velocity of $1500\text{--}2000 \text{ km s}^{-1}$ was determined, which is small for a SN. In addition, the bipolar appearance became stronger, and the nature of this source is now less clear (Beswick et al. 2006).

7. Supernova space VLBI in the context of VSOP-2

From the optically identified SNe studied so far with VLBI, four had flux densities peaking at $\sim 100 \text{ mJy}$ when they became optically thin: SN 1986J, SN 1987A, SN 1993J, SN 1996cr. Their sizes ranged from 0.55 to 2.8 mas at these times (see Table 1). VLBI observations with VSOP-2 would allow making detailed images of such SNe starting at the earliest possible time when the optical depth decreases below unity and the SN becomes optically thin. ‘‘Filming’’ in radio the earliest stages of a SN evolution promises to add invaluable information to our understanding of the aftermath of the explosion.

References

- Bandiera, R., Pacini, F., & Salvati, M. 1984, *ApJ*, 285, 134
 Bartel, N. 1985, *Lecture Notes in Physics*, Berlin Springer Verlag, Vol. 224, *Supernovae as distance indicators*; Proceedings, ed. N. Bartel, 107

- Bartel, N., & Bietenholz, M. F. 2003, *ApJ*, 591, 301
— 2008, *ApJ*, 682, in press
Bartel, N., Bietenholz, M. F., & Rupen, M. P. 1995, *Proc. Natl. Acad. Sci.*, 92, 11374
Bartel, N., et al. 2000, *Science*, 287, 112
— 2002, *ApJ*, 581, 404
Bartel, N., et al. 1994, *Nat*, 368, 610
Bartel, N., Bietenholz, M. F., Rupen, M. P., & Dwarkadas, V. V. 2007, *ApJ*, 668, 924
Bartel, N., et al. 1987, *ApJ*, 323, 505
Bartel, N., Rogers, A. E. E., Shapiro, I. I., Gorenstein, M. V., Gwinn, C. R., Marcaide, J. M., & Weiler, K. W. 1985, *Nat*, 318, 25
Bartel, N., Rupen, M. P., Shapiro, I. I., Preston, R. A., & Rius, A. 1991, *Nat*, 350, 212
Bauer, F. E., Dwarkadas, V. V., Brandt, W. N., Immler, S., Smartt, S., Bartel, N., & Bietenholz, M. F. 2008, *ApJ*, in press (astro-ph/0804.3597)
Beswick, R. J., et al. 2006, *MNRAS*, 369, 1221
Bietenholz, M. F., & Bartel, N. 2007, *ApJ*, 665, L47
Bietenholz, M. F., Bartel, N., & Rupen, M. P. 2001, *ApJ*, 557, 770
— 2002, *ApJ*, 581, 1132
— 2003, *ApJ*, 597, 374
— 2004, *Science*, 304, 1947
— 2005, *Advances in Space Research*, 35, 1052
Bondi, M., Pérez-Torres, M.-A., Dallacasa, D., & Muxlow, T. W. B. 2005, *MNRAS*, 361, 748
Chevalier, R. A. 1982, *ApJ*, 258, 790
Freedman, W. L., et al. 1994, *ApJ*, 427, 628
Gaensler, B. M., Staveley-Smith, L., Manchester, R. N., Kesteven, M. J., Ball, L., & Tzioumis, A. K. 2007, in *American Institute of Physics Conference Series*, Vol. 937, ed. S. Immler & R. McCray, 86
Gallimore, J. F., & Beswick, R. 2004, *AJ*, 127, 239
Granot, J., & Ramirez-Ruiz, E. 2004, *ApJ*, 609, L9
Huterer, D., Sasselov, D. D., & Schechter, P. L. 1995, *AJ*, 110, 2705
Jauncey, D. L., Kembell, A., Bartel, N., Shapiro, I. I., Whitney, A. R., Rogers, A. E. E., Preston, R. A., & Clark, T. A. 1988, *Nat*, 334, 412
Lonsdale, C. J., Diamond, P. J., Thrall, H., Smith, H. E., & Lonsdale, C. J. 2006, *ApJ*, 647, 185
Manchester, R. N., Gaensler, B. M., Wheaton, V. C., Staveley-Smith, L., Tzioumis, A. K., Bizunok, N. S., Kesteven, M. J., & Reynolds, J. E. 2002, *PASA*, 19, 207
Marcaide, J. M., et al. 1994, *ApJ*, 424, L25
Marcaide, J. M., et al. 1995a, *Nat*, 373, 44
Marcaide, J. M., et al. 1995b, *Science*, 270, 1475
Marcaide, J. M., et al. 1997, *ApJ*, 486, L31
Martí-Vidal, I., et al. 2007, *A&A*, 470, 1071
Mioduszewski, A. J., Dwarkadas, V. V., & Ball, L. 2001, *ApJ*, 562, 869
Montes, M. J., Weiler, K. W., Van Dyk, S. D., Panagia, N., Lacey, C. K., Sramek, R. A., & Park, R. 2000, *ApJ*, 532, 1124
Neff, S. G., Ulvestad, J. S., & Teng, S. H. 2004, *ApJ*, 611, 186
Paragi, Z., Kouveliotou, C., Garrett, M. A., Ramirez-Ruiz, E., van Langevelde, H. J., Szomoru, A., & Argo, M. 2007, *The Astronomer's Telegram*, 1215, 1
Pérez-Torres, M. A., et al. 2005, *MNRAS*, 360, 1055
Soderberg, A. M., et al. 2008, *Nature*, 453, 469
Soderberg, A. M., Kulkarni, S. R., Berger, E., Chevalier, R. A., Frail, D. A., Fox, D. B., & Walker, R. C. 2005, *ApJ*, 621, 908
Weiler, K. W., van Dyk, S. D., Discenna, J. L., Panagia, N., & Sramek, R. A. 1991, *ApJ*, 380, 161
Wilkinson, P. N., & de Bruyn, A. G. 1990, *MNRAS*, 242, 529